

Investigation of the Dynamics of Two Chiral Smectogens by Means of  $^2\text{H}$  NMR

Donata Catalano, Mario Cifelli, Marco Geppi, and CarloAlberto Veracini\*

Dipartimento di Chimica e Chimica Industriale, Università degli Studi di Pisa, v. Risorgimento 35, 56126 Pisa, Italy

Received: August 4, 2000; In Final Form: October 12, 2000

In this article we report a dynamics investigation of two chiral smectogens, 1-methylheptyl 4'-(4''-*n*-decyloxybenzoyloxy)biphenyl-4-carboxylate (10B1M7) and [4-(2-methylbutyloxycarbonyl) phenyl] 4-*n*-heptyl-biphenyl carboxylate (MBHB), whose structural and ordering properties were studied previously by our group. The deuterium Zeeman ( $T_{1Z}$ ) and quadrupolar ( $T_{1Q}$ ) spin–lattice relaxation times of two differently deuterated isotopomers of 10B1M7 and one of MBHB have been measured across the whole mesophasic range by means of the broadband Jeener–Broekaert pulse sequence. The trends against temperature of the spectral densities obtained from the relaxation times have been discussed qualitatively in the phases in which the molecules do not align along the external magnetic field, whereas a quantitative interpretation in terms of diffusion coefficients of internal and overall molecular motions has been attempted for the smectic phases for which theoretical models were available. The results obtained for the two smectogens are discussed and compared with those of other smectogens reported in the literature.

## Introduction

Chiral smectogens giving rise to ferroelectric and antiferroelectric phases constitute a class of compounds of great interest because of their possible technological applications. Moreover, many efforts have been made in trying to overcome the difficulties of fully rationalizing the link between their macroscopic behavior and their structural and dynamics microscopic properties. Recently, we investigated the structure and orientational order of two different optically pure chiral smectogens, 1-methylheptyl 4'-(4''-*n*-decyloxybenzoyloxy)biphenyl-4-carboxylate (10B1M7)<sup>1</sup> and [4-(2-methylbutyloxycarbonyl) phenyl] 4-*n*-heptyl-biphenyl carboxylate (MBHB)<sup>2</sup> by means of  $^2\text{H}$  NMR spectroscopy. Two different isotopomers of 10B1M7, deuterated on either the phenyl or biphenyl moieties, were purposely synthesized, whereas a molecule fully deuterated on the biphenyl group was available in the MBHB. Different behavior of the two compounds within the magnetic field was clearly observed. In 10B1M7 the molecules progressively tilt with respect to the magnetic field as the smectic C\* phase is entered on cooling. On the contrary, for MBHB a 13° temperature range of an unwound smectic C\* phase ( $u - S^*$ ) is present below the smectic A, given by the tilt of the smectic layers, rather than of the molecules, from the magnetic field direction.

To better understand the behavior of chiral smectogens, and, in particular, of the rich polymorphism giving rise to several subsmectic C\* phases, a combined analysis of the structural and dynamic properties must be performed. Some points in particular need to be unravelled. One concerns the rotation of the whole molecule around its molecular long axis (spinning motion), which is believed to be highly restricted in ferroelectric phases. The possibility, moreover, of a high hindering of the spinning with respect to the tumbling motion in the smectic A phase of chiral liquid crystals has been proposed recently.<sup>3</sup> The second point deals with the structural and dynamic behavior of the chain containing the chiral center, which can be strongly

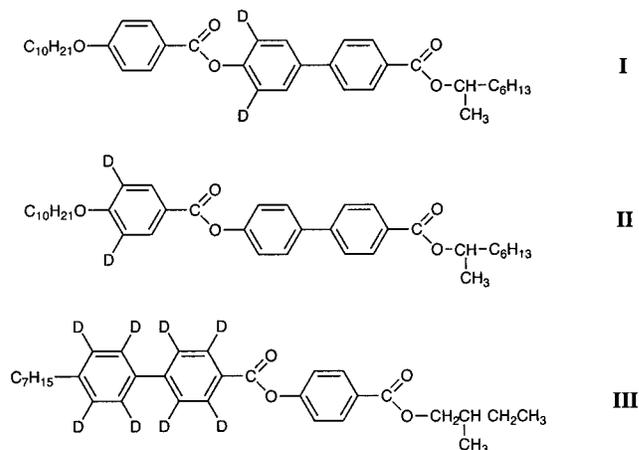


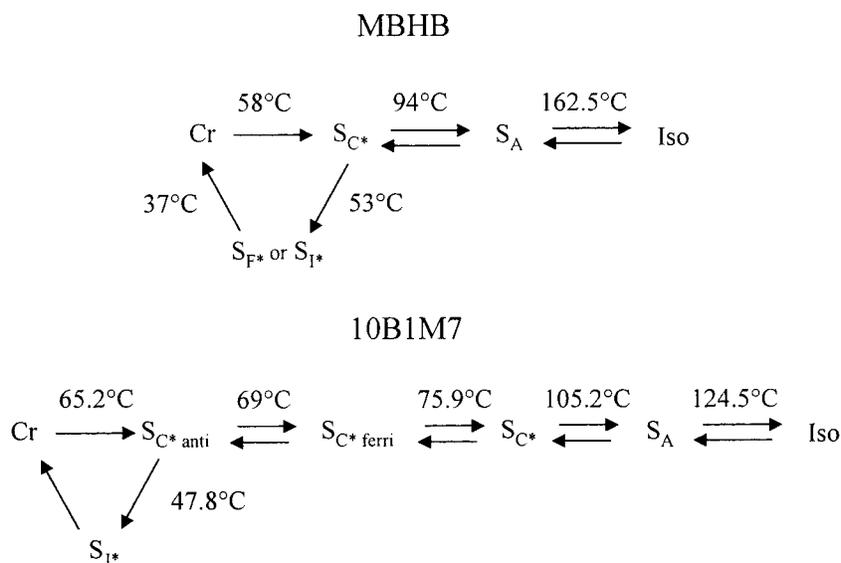
**Figure 1.** Chemical structure of 10B1M7- $d_2$  (I and II) and MBHB- $d_8$  (III).

bent with respect to the molecular long axis and motionally hindered, thus also affecting the spinning motion mentioned above.<sup>4</sup>

We report here a study of the dynamics of MBHB and 10B1M7 based on the measurement of deuterium spin–lattice Zeeman ( $T_{1Z}$ ) and quadrupolar ( $T_{1Q}$ ) relaxation times. These experimental quantities and the connected spectral densities implicitly contain all the dynamic information. Therefore, their interpretation can be attempted by analyzing the spectral densities in terms of suitable theoretical models, which allow individual diffusional coefficients to be obtained for specific internal and overall molecular motions. Models that apply to a variety of cases have been devised,<sup>5–9</sup> but unfortunately none is currently available for tilted smectic C\* phases. Moreover, greater experimental efforts should be required to highlight the molecular dynamics in the tilted phases than in those in which molecules are aligned with the magnetic field. Therefore, in the tilted smectic phases, we shall limit the discussion to a qualitative analysis of the spectral densities, whereas a quantitative application of the available diffusional models will be reported in the smectic A and unwound smectic C\* phases.

\* E-mail: verax@ccci.unipi.it.

## SCHEME 1



## Experimental Section

The optically pure MBHB and 10B1M7 isotopomers investigated, available from previous studies, and shown in Figure 1, exhibit the phase transitions reported in Scheme 1.

<sup>2</sup>H NMR spectra of the samples had been recorded previously.<sup>1,2</sup> The spectra of all compounds show a large deuterium quadrupolar splitting. Moreover, in the proton-coupled spectra of **I** and **II**, the components of the quadrupolar doublet are split by the *ortho*–*meta* deuteron–proton dipolar coupling, whereas, in the spectra of **III**, they show a more complex shape, because of small differences between the quadrupolar splittings of the deuterons on the biphenyl fragment and various small dipolar interactions. This was verified by simulating the experimental line shape by an adapted version of the LEQUOR computer program.<sup>10</sup>

<sup>2</sup>H Zeeman ( $T_{1Z}$ ) and quadrupolar ( $T_{1Q}$ ) spin–lattice relaxation times were measured, under proton decoupling, using a broadband version of the Jeener–Broekaert pulse sequence,<sup>11</sup>  $90_0-2\tau_1-67.5_{270}-2\tau_1-45_{90}-\tau_1-45_{90}-\tau_2-45_0$ , where  $\tau_1$  is a delay of 8.5  $\mu$ s, experimentally determined to optimize the inversion of one component of the quadrupolar doublet when  $\tau_2$  vanishes;  $\tau_2$  is a variable delay time, ranging from 20  $\mu$ s to 200 ms. The sum ( $M_+$ ) and difference ( $M_-$ ) of the integrals of the two components of a quadrupolar doublet, reported as a function of  $\tau_2$ , give  $T_{1Z}$  and  $T_{1Q}$ , respectively, through the two fitting equations:

$$M_+(\tau_2) = a \left[ 1 - b \exp\left(-\frac{\tau_2}{T_{1Z}}\right) \right] \quad (1)$$

$$M_-(\tau_2) = c + d \exp\left(-\frac{\tau_2}{T_{1Q}}\right) \quad (2)$$

which differ slightly from those predicted theoretically<sup>12</sup> to take account of both incomplete inversion at vanishing variable delays and small spectral asymmetries.<sup>13</sup>

Deuterium NMR experiments were performed for the three samples at variable temperature across the whole mesophasic range. A Varian VXR-300 spectrometer, working at 46.04 MHz for deuterium, was used. The 90-degree pulse was 21  $\mu$ s. A relaxation delay of 200 ms and a number of acquisitions of 800, 2000, and 200 for samples **I**, **II**, and **III**, respectively, were

used in the relaxation measurements, depending on the amount of sample available and on the number of deuterons per molecule. Temperature was controlled within 0.1 °C. To check a possible dependence of the results on the spectrometer features, some measurements were repeated using a Bruker AMX-300 spectrometer with a 90-degree pulse of 10  $\mu$ s; the two series of spectra gave consistent results for  $T_{1Z}$  and  $T_{1Q}$ .

## Theory

The following relationships link the experimental relaxation times  $T_{1Z}$  and  $T_{1Q}$  to the spectral densities  $J_1(\omega_0)$  and  $J_2(2\omega_0)$ :

$$\frac{1}{T_{1Z}} = J_1(\omega_0) + 4J_2(2\omega_0) \quad (3)$$

$$\frac{1}{T_{1Q}} = 3J_1(\omega_0) \quad (4)$$

where  $\omega_0/2\pi$  is the Larmor frequency.

Spectral densities contain all the dynamic information, but in a quite implicit form. Therefore it would be useful to express them in terms of other quantities that can discriminate the contributions to the relaxation arising from different motional processes. In fact, the complex dynamics of liquid crystals is characterized by the combined effect of three types of motions: overall reorientations of the whole molecule, internal rotations or jumps of segments of the molecule, and collective motions.

Several theoretical models have been proposed to describe the overall motions of cylindrical molecules in uniaxial phases, the most important being the *small-step rotational diffusion* model by Nordio and Busolin,<sup>5</sup> the *anisotropic viscosity* model by Polnaszek and Freed,<sup>6</sup> and the *third-rate* extension of the latter by Vold and Vold,<sup>7</sup> to which in this article we will refer as “Nordio”, “Freed”, and “Vold” models, respectively. Moreover, additional models have been proposed to take into account either asymmetric molecules in uniaxial phases<sup>8</sup> or uniaxial molecules in biaxial phases with  $D_{2h}$  symmetry.<sup>9</sup> In this work we deal with two types of phases, in which molecules are either aligned ( $S_A$  and  $u - S_C^*$ ) or tilted (various subphases of the smectic  $C^*$  and more ordered smectic phases) with respect to the external magnetic field. In the first case the models for cylindrical molecules in uniaxial phases can be applied confi-

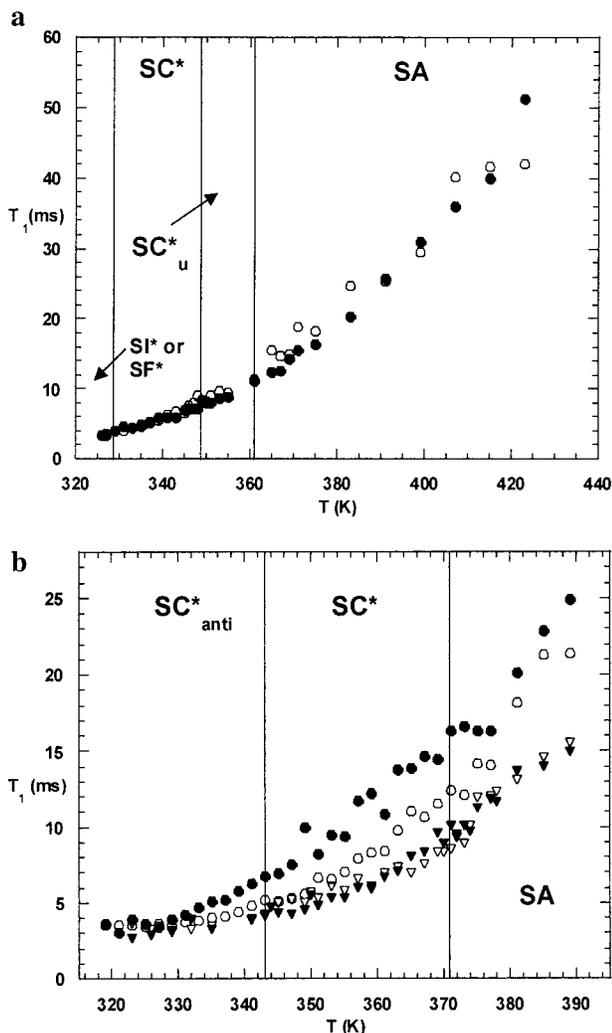


**Figure 2.** (a)  $^2\text{H}$  Zeeman (empty circles) and quadrupolar (full circles) spin–lattice relaxation times of MBHB as a function of temperature; the uncertainties increase from 0.2 to 6 ms with increasing temperature. (b)  $^2\text{H}$  Zeeman (empty symbols) and quadrupolar (full symbols) spin–lattice relaxation times of 10B1M7 as a function of temperature. Circles refer to sample I (deuterated on the biphenyl fragment) and triangles to sample II (deuterated on the phenyl fragment). The uncertainties increase from 0.1 to 3 ms with increasing temperature.

dently, because molecular biaxiality has been estimated to be substantially negligible.<sup>1,2</sup> In the second case, however, no models suitable for relaxation times analysis have been proposed yet. Therefore, we will focus here on the models that have been used to treat the dynamics in the first type of phases.

Internal motions, in particular rotation of the aromatic fragments about their *para* axes, will be considered decoupled from the overall reorientations of molecules.

Collective motions can contribute in principle to spin–lattice deuterium relaxation. Theories exist that describe the contribution to the spectral densities of order director fluctuations, considering them not coupled to reorientational motions. Such a contribution is predicted to vanish for  $J_2(2\omega_0)$  and to show a typical frequency dependence for  $J_1(\omega_0)$ .<sup>14</sup> However, not only is the contribution to  $J_1(\omega_0)$  usually very small in smectic phases at the usual Larmor frequencies of the order of MHz,<sup>15,16</sup> but it is also proportional to the geometrical term  $(3 \cos^2 \beta - 1)^2$ , where  $\beta$  is the angle formed by the C–D bond and the long axis of the rigid fragment under examination; such a factor is almost vanishing for aromatic deuterons, for which  $\beta \approx 60^\circ$ . For this reason the influence of order director fluctuations on aromatic

spectral densities can be neglected here.<sup>17</sup> Other kinds of collective motions take place in smectic C\* phases, because of the formation of an helicoidal structure through the smectic planes, known as Goldstone and soft modes, which represent fluctuations of the helix about the azimuthal and tilt angles, respectively.<sup>18</sup> These too are low-frequency motions and should not affect the spectral densities at 46.04 and 92.08 MHz.

To find an expression of the spectral densities in terms of individual motional parameters, such as diffusional coefficients  $D_i$ , we must adopt an expression for the autocorrelation functions  $g_{m_L m_M}(t)$  relative to the overall molecular motions. Agostini et al. originally used a single-exponential approximation,<sup>19</sup> but subsequently Vold and Vold considered a more suitable sum of decreasing exponential functions<sup>7</sup>:

$$g_{m_L m_M}(t) = c_{m_L m_M} \sum_j a_{m_L m_M}^{(j)} \exp\left(-\frac{t}{\tau_{m_L m_M}^{(j)}}\right) \quad (5)$$

The corresponding spectral densities can thus be obtained as the Fourier transforms of such autocorrelation functions. The spectral densities  $J_{m_L m_M}$  are then combined in an expression giving the experimental quantities  $J_{m_L}$  which appear in eqs 3 and 4.<sup>7</sup> Before these last two steps, the rotation of the aromatic fragment about its *para* axis must also be taken into account for aromatic deuterons. This can be done by “superimposing” the internal motion on the overall molecular motion, that is by taking the product of the respective autocorrelation functions. If the internal motion is considered obeying the strong collision model,<sup>20</sup> the spectral densities can be written eventually as:<sup>21</sup>

$$J_{m_L}(m_L \omega_0) = \frac{3\pi^2}{2} (\nu_q)^2 \sum_{m_M=-2}^2 \sum_{m_R=-2}^2 c_{m_L m_M} [d_{m_R 0}^2(\beta_{R, Q_R})]^2 \times [d_{m_M m_R}^2(\beta_{M, R})]^2 \sum_j a_{m_L m_M}^{(j)} \frac{(\tau_{m_L m_M}^{(j)})^{-1} + (1 - \delta_{m_R}) D_R}{(m_L \omega_0)^2 + [(\tau_{m_L m_M}^{(j)})^{-1} + (1 - \delta_{m_R}) D_R]^2} \quad (6)$$

Here  $\nu_q$  is the quadrupolar coupling constant,  $d_{rs}^2$  are the reduced Wigner matrices,  $\beta_{R, Q_R}$  is the angle between the C–D bond and the *para* axis of the aromatic fragment,  $\beta_{M, R}$  is the angle between this axis and the molecular long axis, and  $D_R$  is the diffusion coefficient relative to the internal rotation of the aromatic fragment about its *para* axis. The time constants  $\tau_{m_L m_M}^{(j)}$  can be expressed as a function of the diffusional coefficients, depending on the model chosen for describing the overall molecular motions. In particular, for Nordio, Freed and Vold models,  $\tau_{m_L m_M}^{(j)}$  can be written as reported in eqs 7, 8, and 9, respectively:

$$\frac{1}{\tau_{m_L m_M}^{(j)}} = \frac{6D_\perp}{b_{m_L m_M}^{(j)}} + m_M^2 (D_\parallel - D_\perp) \quad (7)$$

$$\frac{1}{\tau_{m_L m_M}^{(j)}} = \frac{6D_\beta}{b_{m_L m_M}^{(j)}} + m_L^2 (D_\alpha - D_\beta) \quad (8)$$

$$\frac{1}{\tau_{m_L m_M}^{(j)}} = \frac{6D_\beta}{b_{m_L m_M}^{(j)}} + m_L^2 (D_\alpha - D_\beta) + \xi(m_M) D_\gamma \quad (9)$$

The coefficients  $a_{m_L m_M}^{(j)}$ ,  $b_{m_L m_M}^{(j)}$  and  $c_{m_L m_M}$ , which appear in eqs 5–9 have been calculated and reported in ref 7 as a function of the principal order parameter for a Maier–Saupe potential.

In both Nordio and Freed models the reorientational molecular motions are treated as small-step rotational diffusions in the presence of an ordering Maier–Saupe potential; but, whereas in the Nordio model the motion is described by a diffusion tensor that is diagonal in a molecular fixed frame, in the Freed model the diffusion tensor is diagonal in the laboratory frame.  $D_{\parallel}$  and  $D_{\perp}$  represent the principal components of the diffusion tensor in the Nordio model and describe the motions of spinning and tumbling of the molecular long axis, respectively.  $D_{\alpha}$  and  $D_{\beta}$  ( $\equiv D_{\perp}$ ) represent the principal components of the diffusion tensor in the Freed model, and correspond to the precession and tumbling motions of the molecular long axis in the laboratory frame. When the principal order parameter, which affects the values of the coefficients  $a_{m_1 m_M}^{(j)}$ ,  $b_{m_1 m_M}^{(j)}$ , and  $c_{m_1 m_M}$ , is very high (for instance, 0.9), the rotation diffusion problem becomes insensitive to the choice of the frame in which the rotation diffusion tensor is diagonalized and the Nordio and Freed models can be used indifferently. The Vold model is an extension of the Freed model, in which an additional motion, referred to as  $\gamma$  motion, is taken into account and considered independent of the  $\alpha$  and  $\beta$  motions. If the strong collision model is used for the  $\gamma$  motion, in eq 9,  $\xi(m_M)$  is  $(1 - \delta_{m_M})$ , whereas  $\xi(m_M) = m_M^2$  for small step diffusion.<sup>22</sup>

### Results and Discussion

The deuterium spin–lattice relaxation times  $T_{1Z}$  and  $T_{1Q}$ , measured at variable temperatures by means of the broadband Jeener–Broekaert pulse sequence, are shown in Figure 2 for MBHB (325–423 K) and 10B1M7 (319–389 K). Relaxation measurements have been performed over the whole mesophasic range, with the exception of the most ordered smectic phases (smectic F\* or I\* in MBHB and smectic J\* in 10B1M7) because of the dramatic line broadening that occurs in these cases.<sup>1,2</sup> The two relaxation times are of the order of some milliseconds, and  $T_{1Z} \approx T_{1Q}$  for each deuteron of the two samples at each temperature. Moreover, the increasing trend of relaxation times with increasing temperature indicates a motional narrowing regime ( $\omega_0 \tau_c \ll 1$ ) for the motions mainly contributing to the relaxation, which are therefore fast motions with correlation times shorter than  $10^{-8}$  s. These features are usually found for aromatic deuterons in nematic and less ordered smectic phases. No jumps or evident changes in the relaxation time trends can be observed at the phase transitions for both liquid crystals.

We can try to improve our analysis of the dynamics by looking at the spectral densities  $J_1(\omega_0)$  and  $J_2(2\omega_0)$  obtained from the measured relaxation times by means of eq 3 and 4. The logarithmic plots of  $J$  against  $1000/T$ , reported in Figure 3, in all cases highlight regular linear trends. No discontinuities can be revealed except that for the  $J_2$  trends of both phenyl and biphenyl deuterons of 10B1M7, the slope of which substantially decreases to less than 343 K, that is in the  $S_{\text{antiferro}}^*$  phase. This may indicate some changes in the “fast” dynamics, but also the occurrence of a tilt angle between the local molecular director and the magnetic field is expected to contribute to this effect, as can be estimated roughly following ref 15, for instance. Such a contribution might be negligible for compound **III**, which exhibits a tilt angle of about 15 degrees,<sup>2</sup> and appreciable for compounds **I** and **II**, where the tilt angle reaches about 27 degrees.<sup>2,23</sup> Changes in the slower, collective motional processes should also occur below the  $S_A - S_C^*$  transition, but they could not affect spin–lattice relaxation times. In effect, the previous studies performed on both MBHB<sup>2</sup> and 10B1M7<sup>1</sup> highlighted a remarkable increase of the <sup>2</sup>H line width, which is mainly

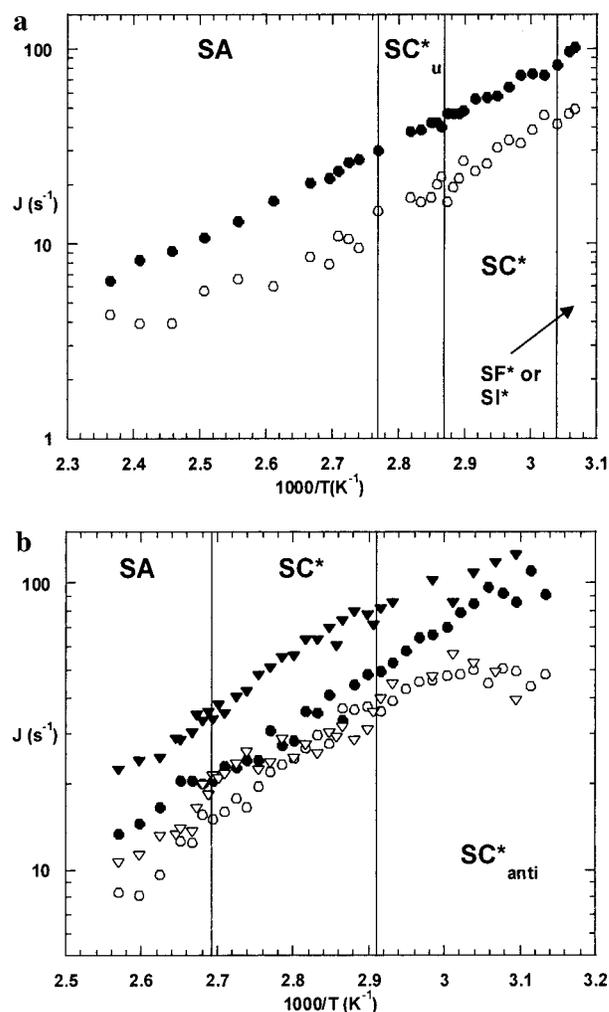


**Figure 3.** Logarithmic plots of the spectral densities  $J_1(\omega_0)$  (full symbols) and  $J_2(2\omega_0)$  (empty symbols) of MBHB (a) and 10B1M7 (b) vs  $1000/T$ . The same symbols as in Figure 2 have been used. In all cases the estimated uncertainty is between 1 and 5  $s^{-1}$ ; typical values are 1–2  $s^{-1}$ .

influenced by motions in the kHz regime, at the onset of the smectic C\* phase and in the more ordered smectic phases.

As stated previously in the theory section, a more detailed interpretation of the deuterium spin–lattice relaxation times could be given just for the  $S_A$  and  $u - S_C^*$  phases through theoretical models that express the spectral densities in terms of diffusional coefficients. To this aim, the experimental spectral densities were fitted by eq 6 combined with eq 7 or 8. The  $\beta_{M,R}$  angle was always fixed to the standard value of  $60^\circ$ . The  $\beta_{R,Q_R}$  angle was 0 for compounds **II** and **III**, for which the *para* axis of the deuterated fragment was considered parallel to the molecular long axis. For compound **I**  $\beta_{M,R}$  was fixed to  $14.5^\circ$ , which is the value of the angle between the *para* axes of the phenyl and biphenyl fragments.<sup>1</sup> As already noted, the coefficients  $a_{m_1 m_M}^{(j)}$ ,  $b_{m_1 m_M}^{(j)}$  and  $c_{m_1 m_M}$  are given in ref 7 as a function of the principal order parameter, the values of which are reported for the compounds under examination in refs 1 and 2 in the temperature ranges studied here. In the fitting of the spectral densities to obtain diffusional coefficients, in principle, two different strategies are possible: either performing a fitting and determining the diffusion coefficients at each temperature (“single-point” approach) or imposing an Arrhenius trend for the diffusion coefficients against temperature and performing a simultaneous fitting of the experimental data at all temperatures

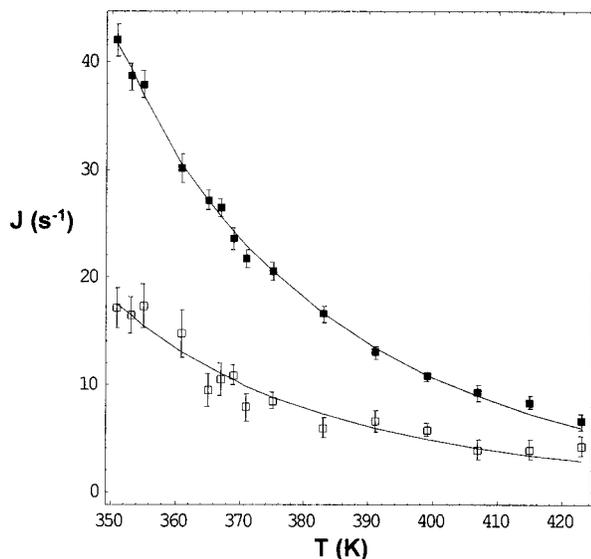


**Figure 4.** Experimental and fitted spectral densities of MBHB. Full and empty squares refer to  $J_1(\omega_0)$  and  $J_2(2\omega_0)$ , respectively.

(“global-target” approach). In the global-target approach the parameters to be obtained will be one preexponential coefficient ( $D_\infty^i$ ) and one activation energy ( $E_a^i$ ) for each motion taken into account by the model.

The relaxation data have been analyzed using a suitable software based on a nonlinear least-squares fit routine, minimizing the sum-squared errors, or the quality factor  $Q$ , defined by:

$$Q = \frac{\sum_i (J_i^{\text{calc}} - J_i^{\text{exp}})^2}{\sum_i (J_i^{\text{exp}})^2} \cdot 100 \quad (10)$$

**MBHB.** We had one deuterated site for MBHB, and therefore two experimental spectral densities for each temperature, whereas the models that we have taken into account provide at least three diffusion coefficients to be determined (spinning or precession, tumbling, and internal rotation of the aromatic fragment around its *para* axes), thus making the global-target

method mandatory. Moreover, given the absence of discontinuities or slope changes in the spectral densities trends vs temperature at the  $S_A - uS_C^*$  transition, we decided to impose the same Arrhenius parameters in the two phases, analyzing all the data available in both  $S_A$  and  $u - S_C^*$  ranges at the same time, thus exploiting the availability of experimental data over a relatively large temperature range of almost 80°.

A first attempt at fitting the experimental spectral densities by means of Nordio and Freed models without considering the internal motion was performed, but this did not allow good reproduction of experimental data, thus confirming the decisive contribution of this motion to the  $^2\text{H}$  spin-lattice relaxation. Fittings of very good quality ( $Q \approx 0.25$ , see Figure 4 as an example) were obtained by using the Nordio model for overall molecular motions and the strong collision model for the internal rotation of the biphenyl fragment. However, comparable  $Q$  values, corresponding to different sets of best-fit parameters,  $D_\infty^i$  and  $E_a^i$ , and to very similar reproduction of the experimental spectral densities, could be reached starting from different initial values for the fitting parameters. In spite of this, some important conclusions could be drawn from a deep data analysis:  $D_{\parallel}$  and  $D_R$  are always between  $9 \cdot 10^8$  and  $2 \cdot 10^{10} \text{ s}^{-1}$  throughout the temperature range investigated, whereas values of  $D_{\perp}$  up to  $2 \cdot 10^9 \text{ s}^{-1}$  are compatible with the experimental data, strongly different values of  $D_{\perp}$  being compensated by minor changes of  $D_{\parallel}$  and  $D_R$ . Diffusion coefficient trends against temperature corresponding to three cases with very different  $D_{\perp}$  values are shown in Figure 5.

Because the principal order parameter is less than 0.79 at each temperature involved in our analysis, we also tested the Freed model, which gives substantially the same results presented above for the Nordio model. This is not surprising considering that  $D_\beta \equiv D_{\perp}$ ,  $D_R$  refers to the same motion and only  $D_\alpha$  and  $D_{\parallel}$  correspond, in principle, to different motions.

**10B1M7.** The availability of two differently deuterated molecules for 10B1M7 allowed us to measure four different spectral densities at each temperature. Unfortunately, in this case, a much narrower  $S_A$  range (about 20 °C) and no  $u - S_C^*$  phase are present. A single-point procedure could be applied in principle by solving a system of four equations, because four diffusional coefficients should be determined using Nordio and

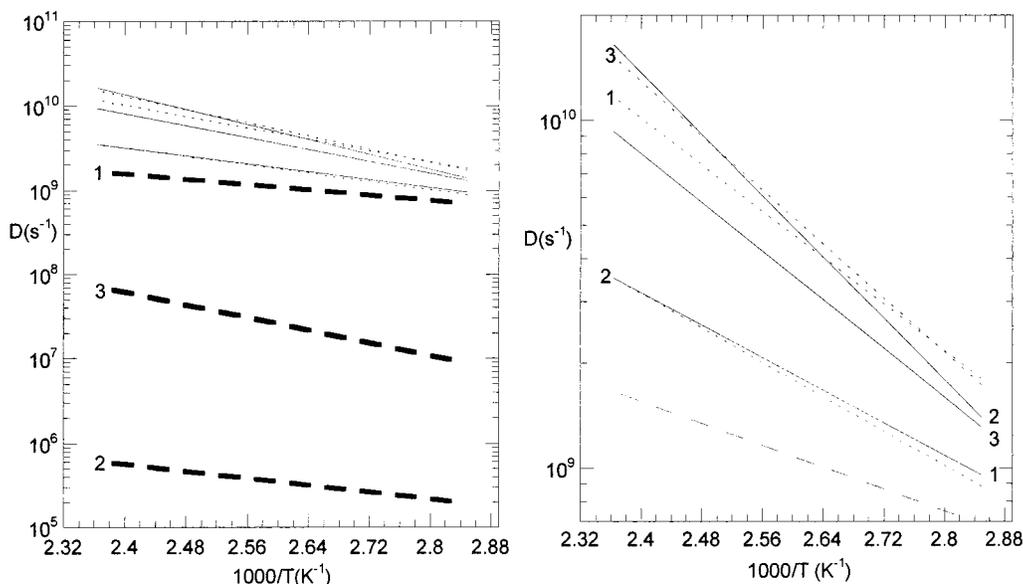


**Figure 5.** Logarithmic plots of the diffusion coefficients obtained for MBHB using the Nordio model vs  $1000/T$ . Solid, dashed, and dotted lines refer to  $D_{\parallel}$ ,  $D_{\perp}$ , and  $D_R$ , respectively.

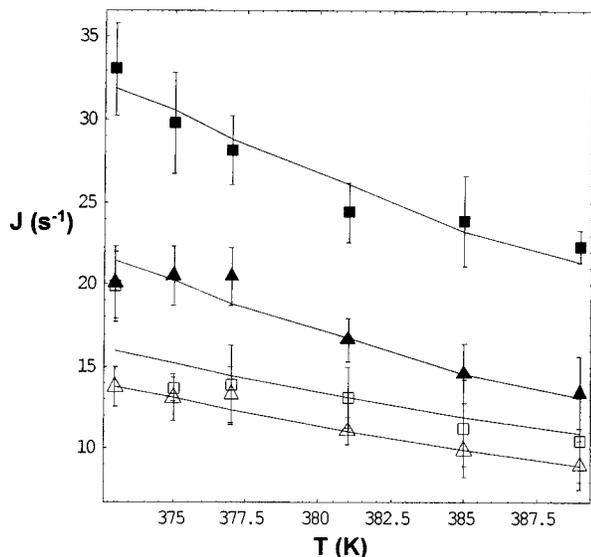


**Figure 6.** Experimental and fitted spectral densities of 10B1M7. Full and empty symbols indicate  $J_1(\omega_0)$  and  $J_2(2\omega_0)$ , respectively; triangles refer to sample I and squares to sample II.

Freed models, two relative to spinning ( $D_{||}$ ) or precession ( $D_{\alpha}$ ) and tumbling ( $D_{\perp}$ ) molecular motions and two for the internal rotations of the deuterated aromatic fragments ( $D_{R1}$  and  $D_{R2}$ , relative to biphenyl and phenyl fragments, respectively). The uncertainties on diffusional coefficients obtained following this procedure would be remarkably higher than those produced by a global-target fitting, owing to the non-negligible error present on experimental relaxation times; therefore, we applied this last method even for 10B1M7.

As in MBHB, a good fitting of the spectral densities could not be performed without taking into account internal rotations. The fitting procedure based on the Nordio and strong collision models for overall and internal motions, respectively, gave a good reproduction of the experimental spectral densities with quite low  $Q$  values of about 0.45 (see Figure 6). The results are in agreement with those found for MBHB, with  $D_{||}$ ,  $D_{R1}$ , and  $D_{R2}$  between  $7 \cdot 10^8$  and  $6 \cdot 10^9$  s<sup>-1</sup> throughout the smectic A range investigated and  $D_{\perp}$  with an upper limit at  $6 \cdot 10^9$  s<sup>-1</sup>, but

substantially indetermined below this limit. Diffusion coefficient trends against temperature corresponding to three cases with very different  $D_{\perp}$  values are reported in Figure 7. In all cases, the rotation about the *para* axis is faster for the biphenyl than for the phenyl fragment. Again, the use of the Freed model instead of the Nordio model gave analogous results.

Some considerations should be made concerning both MBHB and 10B1M7. First of all, it must be pointed out that the use of either Nordio or Freed models, in combination with strong collision for internal rotations, gives rise to an excellent reproduction of the experimental spectral densities, thus making the attempt to use the Vold model useless, which adds one more diffusion coefficient, that is two fitting parameters, to the Freed model. This can introduce a remarkably higher uncertainty in the determination of single diffusional coefficients.

Despite the indeterminacy of  $D_{\perp}$ , it is possible to give a reliable estimate of the order of magnitude of all the other diffusion coefficients (see Figures 5 and 7). The comparison of our results with those obtained by <sup>2</sup>H NMR for other liquid crystals reveals a good agreement between the values found for  $D_{||}$ ,  $D_{\alpha}$ , and  $D_R$ .<sup>24</sup> This suggests that the chirality of the molecules does not particularly affect the spinning motion.  $D_{\perp}$  (or  $D_{\beta}$ ) is usually smaller than  $D_{||}$  and  $D_R$ , even though, at least in one case, the possibility of  $D_{\perp} \gg D_{||}$  has been proposed.<sup>3</sup> In our cases, the upper limits found for  $D_{\perp}$  rule out the occurrence of tumbling motions much faster than spinning ones. The results shown here, relative to two different experimental data sets, strongly suggest that the problem of the indeterminacy of the diffusion coefficient relative to the tumbling motion could be more general and might not have been recognized yet. On the other hand, such indeterminacy could be removed performing measurements at different Larmor frequencies and/or at variable orientations between the phase director and the external magnetic field.<sup>25</sup> In any case, a comparison with findings from different techniques can be helpful: dielectric relaxation measurements performed in the  $S_A$  phase of similar ferroelectric liquid crystals yielded values at least 3 orders of magnitude smaller for the characteristic frequency of the tumbling motion than for that of the spinning motion.<sup>26</sup> Moreover, the frequency values reported give correlation times of about  $10^{-8}$ – $10^{-9}$  and

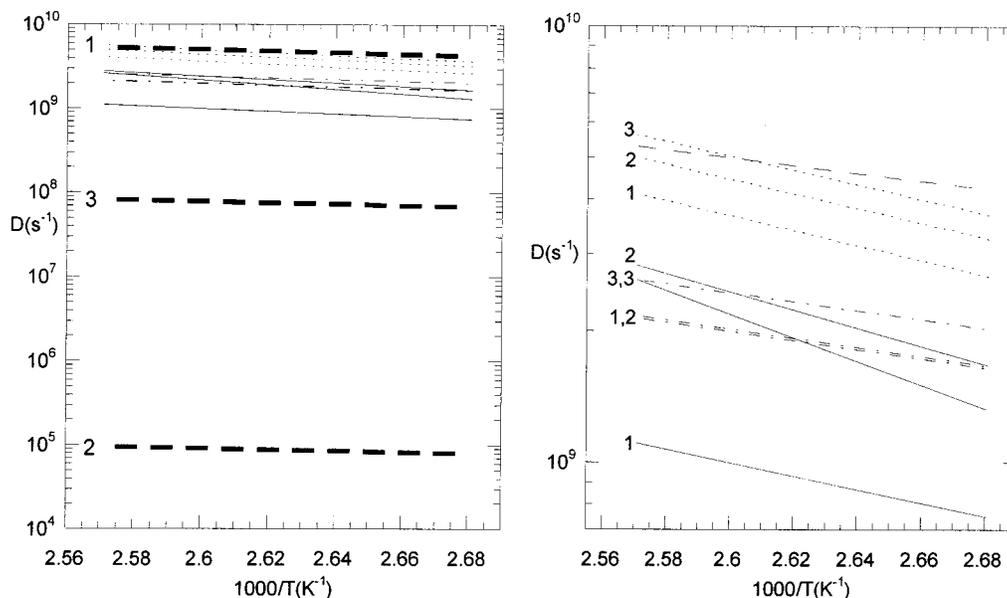


**Figure 7.** Logarithmic plots of the diffusion coefficients obtained for 10B1M7 using the Nordio model vs  $1000/T$ . Solid, dashed, dotted, and dot-dashed lines refer to  $D_{||}$ ,  $D_{\perp}$ ,  $D_{R1}$ , and  $D_{R2}$ , respectively.

$10^{-5}$  s for the spinning and tumbling motions, respectively, which are compatible with our results.

## Conclusions

Deuterium Zeeman and quadrupolar spin–lattice relaxation times have been measured in the smectic A and smectic C\* phases of partially deuterated samples of MBHB and 10B1M7 and were affected mainly by fast ( $\tau_c < 10^{-8}$  s) molecular and internal reorientational motions. No discontinuities in the spectral density trends could be revealed throughout the temperature range investigated, with the exception of  $J_2(2\omega_0)$  in 10B1M7 at about 343 K, thus supporting the hypothesis that some changes in the fast dynamics could occur in the chiral chain at the  $S_C^* - S_{\text{antiferro}}^*$  transition. The understanding of the dynamic properties of these systems could be improved by studying the relaxation properties of the aliphatic chains and by investigating experimental quantities, like line widths, more sensitive to slower collective motions, which are expected to affect the  $S_A - S_C^*$  transition and the occurrence of the various smectic C\* subphases.

A detailed analysis of spectral densities gave a very good reproduction of the experimental data when either the Nordio or Freed models for molecular motions and strong collision for the internal rotation of the aromatic fragments were used. Estimates of the diffusional coefficients relative to the spinning (or precession) and internal motions were obtained in the  $S_A$  and  $u - S_C^*$  phases, but  $D_{\perp}$  (or  $D_{\beta}$ ) was indetermined. This suggests that the analysis of deuterium relaxation data must be performed very cautiously, exploiting, when possible, the frequency and orientation dependence of the relaxation times and comparing the results with those of different techniques.

To better clarify the molecular dynamics in the smectic C\* range, a combined experimental and theoretical effort is necessary to remove the restriction limiting the spectral density analysis to unwound smectic phases.

**Acknowledgment.** The financial support of italian MURST is gratefully acknowledged. The authors thank Dr. C. Forte, ICQEM-CNR of Pisa, for the use of the Bruker spectrometer, as well as Dr. L. Calucci for her contribution in the development of the software used in the data analysis and for the helpful discussion.

## References and Notes

- (1) Catalano, D.; Cavazza, M.; Chiezzi, L.; Geppi, M.; Veracini, C. *Liq. Cryst.* **2000**, *27*, 621.
- (2) Catalano, D.; Cifelli, M.; Fodor-Csorba, K.; Gacs-Baitz, E.; Geppi, M.; Jakly, A.; Veracini, C. A. *Mol. Cryst. Liq. Cryst.* in press.
- (3) Dong, R. Y.; Cheng, M.; Fodor-Csorba, K.; Veracini, C. A. *Liq. Cryst.* **2000**, *27*, 1039.

- (4) Yoshida, S.; Jin, B.; Takanishi, Y.; Tokumaru, K.; Ishikawa, K.; Takezoe, H.; Fukuda, A.; Kusumoto, T.; Nakai, T.; Miyajima, S. *J. Phys. Soc. Jpn.* **1999**, *68*, 9. Jin, B.; Ling, Z.; Takanishi, Y.; Ishikawa, K.; Takezoe, H.; Fukuda, A.; Kakimoto, M.; Kitazume, T. *Phys. Rev. E* **1996**, *53*, 4295. Ouchi, Y.; Yoshioka, Y.; Ishii, H.; Seki, K.; Kitamura, M.; Noyori, R.; Takanishi, Y.; Nishiyama, I. *J. Mater. Chem.* **1995**, *5*, 2297.
- (5) Nordio, P. L.; Busolin, P. *J. Chem. Phys.* **1971**, *55*, 5485. Nordio, P. L.; Rigatti, G.; Segre, U. *J. Chem. Phys.* **1972**, *56*, 2117.
- (6) Polnaszek, C. F.; Freed, J. H. *J. Chem. Phys.* **1975**, *79*, 2283.
- (7) Vold, R. R.; Vold, R. L. *J. Chem. Phys.* **1988**, *88*, 143.
- (8) Tarroni, R.; Zannoni, C. *J. Chem. Phys.* **1991**, *95*, 4550.
- (9) Bergreen, E.; Tarroni, R.; Zannoni, C. *J. Chem. Phys.* **1993**, *99*, 6180.
- (10) Diehl, P.; Kellrhals, H. P.; Niederberger, W. *J. Magn. Reson.* **1971**, *4*, 352. The version of the program LEQUOR used here optimizes dipolar couplings and chemical shifts, given the quadrupolar couplings and experimental lines of the  $^2\text{H}$  NMR spectra of molecules oriented in liquid crystals.
- (11) Wimperis, S. *J. Magn. Reson.* **1990**, *86*, 46.
- (12) Vold, R. L.; Dickerson, W. H.; Vold, R. R. *J. Magn. Reson.* **1981**, *43*, 213.
- (13) Catalano, D.; Ciampi, E.; Fodor-Csorba, K.; Forte, C.; Geppi, M.; Imbardelli, D. *Liq. Cryst.* **1996**, *21*, 927.
- (14) Pincus, P. *Solid State Commun.* **1969**, *7*, 415. Blinc, R.; Hogenboom, D.; O'Reilly, D.; Peterson, E. *Phys. Rev. Lett.* **1969**, *23*, 969.
- (15) Vold, R. L.; Vold, R. R. In *The Molecular Dynamics of Liquid Crystals*; Luckurst, G. R., Veracini, C. A., Eds.; Kluwer Academic: Dordrecht, 1994.
- (16) Sebastiao, P. J.; Ribeiro, A. C.; Nguyen, H. T.; Noack, F. *Z. Naturforsch.* **1993**, *48a*, 851. Ribeiro, A. C. *Mol. Cryst. Liq. Cryst.* **1987**, *148*, 85.
- (17) Barbara, T. M.; Vold, R. R.; Vold, R. L.; Neubert, M. E. *J. Chem. Phys.* **1985**, *82*, 1612. Forte, C.; Geppi, M.; Veracini, C. A. *Z. Naturforsch.* **1994**, *49a*, 311.
- (18) Blinc, R.; Filipic, C.; Levstik, A.; Zeks, B.; Carlson, T. *Mol. Cryst. Liq. Cryst.* **1987**, *151*, 1.
- (19) Agostini, G.; Nordio, P. L.; Rigatti, G.; Segre, U. *Atti Accad. Naz. Lincei, Ser. 8*, **1975**, *13*, 1.
- (20) Beckmann, P. A.; Emsley, J. W.; Luckurst, G. R.; Turner, D. L. *Mol. Phys.* **1986**, *54*, 97.
- (21) Dong, R. Y. *Nuclear Magnetic Resonance of Liquid Crystals*; Springer-Verlag: New York, 1997.
- (22) Woessner, D. E. *J. Chem. Phys.* **1962**, *36*, 1. Dong, R. Y. *Mol. Cryst. Liq. Cryst.* **1986**, *141*, 349.
- (23) Goodby, J. W.; Patel, J. S.; Chin, E. J. *J. Mater. Chem.* **1992**, *2*, 197.
- (24) Dong, R. Y.; Richards, G. M.; Lewis, J. S.; Tomchuk, E.; Bock, E. *Mol. Cryst. Liq. Cryst.* **1987**, *144*, 33. Dong, R. Y. *J. Chem. Phys.* **1988**, *88*, 3962. Forte, C.; Geppi, M.; Veracini, C. A. *Z. Naturforsch.* **1994**, *49a*, 311. Calucci, L.; Geppi, M.; Veracini, C. A.; Forte, C.; Gandolfo, C. *Mol. Cryst. Liq. Cryst.* **1997**, *303*, 415. Calucci, L.; Geppi, M.; Veracini, C. A.; Dong, R. Y. *Chem. Phys. Lett.* **1998**, *296*, 357. Calucci, L.; Catalano, D.; Fodor-Csorba, K.; Forte, C.; Veracini, C. A. *Mol. Cryst. Liq. Cryst.* **1999**, *331*, 9. Dong, R. Y.; Morcombe, C. R.; Calucci, L.; Geppi, M.; Veracini, C. A. *Phys. Rev. E* **2000**, *61*, 1559.
- (25) Barbara, T. M.; Vold, R. R.; Vold, R. L. *J. Chem. Phys.* **1983**, *79*, 6338. Cifelli, M.; Forte, C.; Geppi, M.; Veracini, C. A. *Mol. Cryst. Liq. Cryst.*, in press.
- (26) Buivydas, M.; Gouda, F.; Andersson, G.; Lagerwall, S. T.; Stebler, B.; Bomelburg, J.; Heppke, G.; Gestblom, B. *Liq. Cryst.* **1997**, *23*, 723.